Co-current combustion of oil shale -Part 1 : Characterization of the solid and gaseous products

Marcio F. Martins, Sylvain Salvador, Jean-François Thovert, Gérald Debenest

Co-current combustion of oil shale – Part 1: Characterization of the solid and gaseous products

M.F. Martins [a,*], S. Salvador [a], J.-F. Thovert [b], G. Debenest [c,d]

[a] Université de Toulouse, MINES ALBI, RAPSODEE, UMR CNRS 2392, Albi F 81013, France
[b] LCD, Ecole Nationale Supérieure de Mécanique et d'Aérotechnique, 86961 Futuroscope Chasseneuil cedex, France
[c] Université de Toulouse, INPT, UPS, IMFT, Institut de Mécanique des Fluides de Toulouse, Allée Camille Soula, F-31400 Toulouse, France
[d] CNRS, IMFT, F-31400 Toulouse, France

A B S T R A C T

Co-current combustion front propagation in a bed of crushed oil shale (OS) leads to the production of liquid oil, of a flue gas and of a solid residue. The objective of this paper was to provide a detailed chemical characterization of Timahdit oil shale and of its smoldering combustion products. The amount of fixed carbon (FC) formed during devolatilization is measured at 4.7% of the initial mass of oil shale whatever the heating rate in the range 50–900 K min^{-1}. The combustion of oil shale was operated using a mix of 75/25 wt. of OS/sand with an air supply of 1460 l min^{-1} m^{-2}. In these conditions, not all the FC is oxidized at the passage of the front, but 88% only, with a partitioning of 56.5% into CO and the rest into CO_2. A calorific gas with a lower calorific value of 54 kJ mol^{-1} is produced. Approximately 52% of the organic matter from OS is recovered as liquid oil. The front decarbonates 83% of carbonates.

Keywords:
Oil shale
Combustion front
Chemical characterization

1. Introduction

Oil shales are natural sedimentary rocks present on the surface of the earth as 100–150 m thick layers, sometimes as outcrops or underground. They consist of a mineral porous matrix with the porosity filled with oil, called kerogen, representing 10–65% of the total mass. The mineral matrix consists of carbonates, quartz and clay [1,2].

After mining, the oil shale comes in the form of blocks. When these blocks are crushed, they form a kind of sand. Co-current combustion of oil shale as a porous bed fed by air is worth studying for two main reasons:

(i) From a scientific point of view: the mechanisms to propagate a combustion front involve the chemistry of the transformations of the OS bed and of the oxidation reactions, the heat transfer (due to the high temperature elevation) and the gas flow in the porous bed, with strong couplings. Because of these coupled mechanisms, the structure of a combustion front is complex and can vary depending on a number of parameters. These problems are still not fully understood. The reader can refer to the pioneering work of Palmer [3], to the review of Ohlemiller [4] or to the recent synthesis of Rein [5] for more details about the so called smoldering phenomena. Put simply, the structure of a combustion front and the reactions involved during its propagation are described in Fig. 1. The oil shale dries when it is heated. The organic fraction then devolatilizes and produces volatile matter. Part of this volatile matter will condense to form liquid oil. A solid residue called fixed carbon (FC) is left in the mineral matrix. The energy to heat the medium is brought by the total or partial oxidation of the FC, and potentially of the volatile matter. If the temperature of the combustion front is high, the carbonates in the oil shale are decarbonated, either partly or totally.

A significant advantage of an OS grain bed as a porous medium to study the propagation of a combustion front is that the bed preserves its geometry during the passage of the front, allowing a 1D situation to be maintained. This was the original motivation for using an OS grain bed in this work.

(ii) From an application point of view: propagating a combustion front in a particle bed of OS is a way to recover part of the oil contained in it. The oil recovered can be used as a petroleum-like liquid. Moreover, the flue gas that is produced may prove interesting as a source of energy. The combustion of oil shale can be made *in situ* or in surface processes after mining.

Several studies can be found in the literature of the composition of OS [1,2], [6–8]. The composition of the recovered liquid oil has also been characterized [9–11]. Nevertheless, very few studies have been devoted to the composition of the solid residue after pyrolysis [11]. There is no literature available concerning the flue

* Corresponding author. Tel.: +33 5 63 49 30 26; fax: +33 5 63 49 32 42.
E-mail address: marcio.martins@enstimac.fr (M.F. Martins).

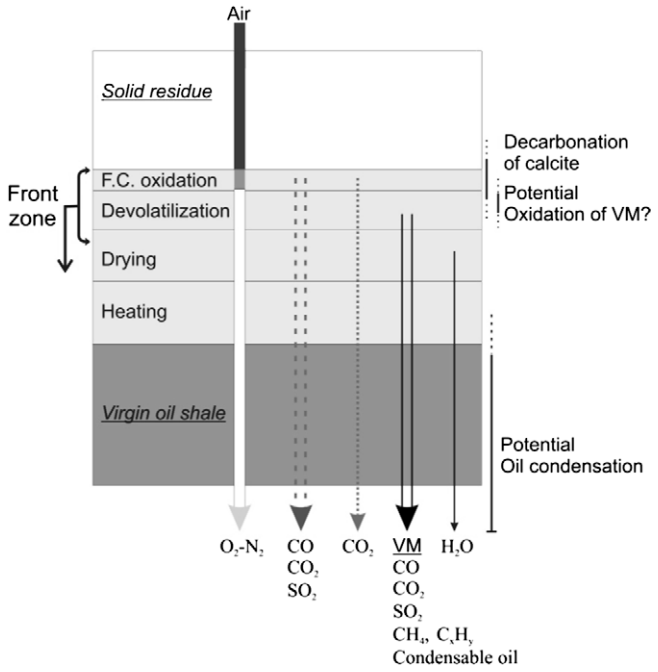

Fig. 1. Description of the main phenomena occurring during the propagation of a combustion front.

gas after combustion, which would provide a global vision of the OS combustion process. Thus, the objective of this work is to provide detailed physical, chemical and thermochemical characterizations of OS before and after combustion, as well as the composition of the flue gas.

The characterization will also provide the answer to a question: are the carbonates constituting the OS decarbonated during the passage of the front? There is an important environmental issue surrounding this question because the carbonate decomposition rate has direct influences on the heating value of the flue gas and on CO_2 emissions [12–14].

This work was also the basis for a parallel study of the structure of the front, Martins et al. [15]. These results, when put together, should constitute a detailed benchmark, enabling the propagation of a combustion front to be modeled in future works.

2. Characterization of oil shale

We used the OS deposit of Timahdit in Morocco. This deposit consists of several layers. The layer "M" was studied here.

2.1. Physical characterization

The oil shale was received as hard dark-grey blocks, typically 10–20 cm long and 10–20 cm wide, and several centimeters thick. The blocks do not have a particular smell and do not dirty the fingers when manipulated. The real density is 2257 kg m^{-3} from H_e pycnometer measurement. Mercury intrusion tests indicated a value of 2244 kg m^{-3}, while measuring a cubic block and weighing it gave 2214 kg m^{-3}. The value of 2214 kg m^{-3} was adopted in this work.

The particle size range 500–1000 μm was obtained after grinding. This range was retained for the analysis and experiments reported here.

From the mass of the oil shale bed in the reactor, the apparent density of a bed was calculated at 1172 kg m^{-3}. The inter-particle porosity of a bed is then 47.0%.

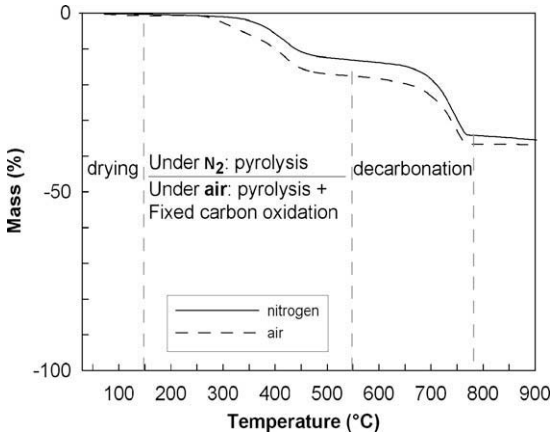

Fig. 2. TGA of oil shale under air and under nitrogen – heating at 3 K min^{-1}.

2.2. Thermogravimetric analysis (TGA) and differential scanning calorimetry analysis (DSC)

A variety of reactions are brought about by the application of heat. For example, [16] reported that the presence of a wide variety of minerals in the oil shale matrix significantly complicates thermal behavior. In general, the following reactions can be identified:

(a) evolution of water and gases;
(b) conversion of kerogen to bitumen;
(c) alteration of bitumen;
(d) dissociation of bitumen from oils, gases and other compounds;
(e) vaporization of oils;
(f) burn-off of fixed carbon;
(g) decomposition of organic residues and inorganic minerals.

The TGA experiments were carried out using a small sample mass – approximately 30 mg – with a small heating rate of 3 K min^{-1} up to 900 °C; complementary tests were performed at 10 K min^{-1}. The flow rate of atmosphere gas was fixed at 33 ml min^{-1}. TG experiments were repeated and showed a good reproducibility, with a maximum deviation of a few%. The decomposition of the oil shale sample, under both inert atmosphere and air, are presented in Fig. 2. Under N_2 atmosphere several stages are indicated:

(a) at temperatures between 50 and 150 °C a mass loss of a few% can be observed. It can be attributed to water evaporation;
(b) in the temperature range 150–550 °C an important mass loss can be observed. The differential scanning calorimetry test performed further (Fig. 4) did not indicate a significant reaction heat. This stage was attributed to kerogen decomposition into volatile matter - including condensable oil - and into solid FC;
(c) in the temperature range 550–770 °C, a last and important mass loss was observed. The differential scanning calorimetry test performed further (Fig. 4) indicated a strongly endothermic reaction. This stage was attributed to the thermal decomposition of carbonates producing carbon dioxide.
(d) during TGA under air, the same sequence is observed, but the mass loss between 150–550 °C is more important. This difference can be attributed to the oxidation of the organic matter remaining as a solid, or fixed carbon. Therefore, the difference between the two mass curves around $T = 550$ °C gives the amount of 4.8% for FC.

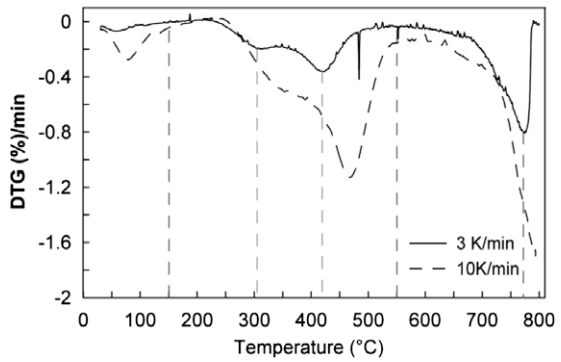

Fig. 3. DTG curves of oil shale under air – heating at 3 and 10 K min^{-1}.

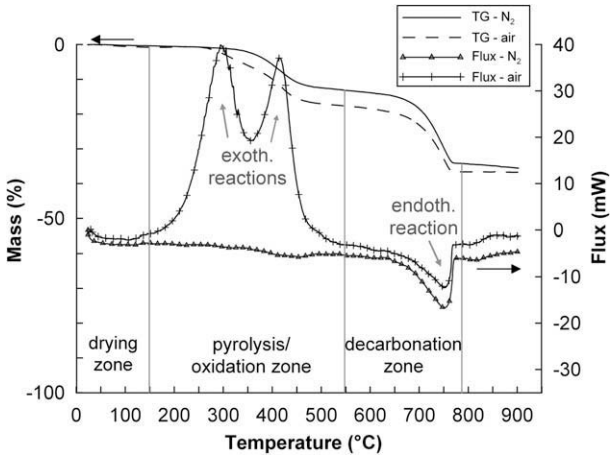

Fig. 4. TGA/DSC of oil shale under air and under nitrogen – heating at 3 K min^{-1}.

There is no clear separation between the two stages of char oxidation and decarbonation along the test. For this reason, it was not possible to determine with any accuracy the amount of organic matter as the mass difference between the dry oil shale and oil shale after oxidation.

It is worth noting that the difference between the two curves decreases along the decarbonation process. This means that for the experiments under N_2, the amount of FC decreases during decarbonation, and even after completion of decarbonation. It is difficult to give a physical explanation to this observation. The total mass loss of the oil shale sample heated to 900 °C under air is 36.7%.

Fig. 3 shows the first derivative curve of sample mass versus temperature, giving the Differential Thermogravimetry (DTG) of oil shale under air at the heating rate of 3 and 10 K min^{-1}. At 3 K min^{-1} first peak is observed at 310 °C; it is usually called the LTO (Low Temperature Oxidation) peak, and is attributed to the oxidation reaction of light hydrocarbons formed by cracking, which are released between 177 and 377 °C depending on the heating rate and oil shale type [17]. The second peak at 420 °C is called the HTO (High Temperature Oxidation) peak. It originates from the oxidation of FC and possibly other components; this is discussed further with the report on DSC tests. The last peak at 770 °C is attributed to the decarbonation process. When the heating rate is increased to 10 K min^{-1}, a peak appears at 60 °C. This phenomenon was also clearly observed during all experiments in the combustion cell, Martins et al. [15], where a temperature plateau can be seen at precisely 60 °C for all thermocouples. These plateaus around 60–80 °C are typical of forward propagation [18].

The DSC tests were carried out in the same experimental conditions as TGA experiments. The results are reported in Fig. 4. The experiment under air shows two exothermic reactions between 250–550 °C. The first peak at 290 °C corresponds to LTO. The second at 410 °C corresponds to HTO. Indeed, these two peaks do not appear when the DSC is performed under N_2 as shown in Fig. 4. The origin of the second peak was investigated by performing a similar analysis with a sample of oil shale previously pyrolyzed under inert atmosphere: only the second peak appears, and it is lower compared to the test with oil shale. This shows that the oxidation of FC is responsible for part of the energy released during HTO. The other species oxidizing during HTO is probably pyrolytic carbon that was deposited at the surface of the solid residue from the oil shale pyrolysis, in the conditions of TG/DSC experiments. For the two exothermic reactions that occur in the range 250–550 °C – that cannot be clearly separated – the reaction heat is +3700 kJ kg^{-1}. The reader can find TGA and DSC based fundamental studies in both pyrolysis and combustion conditions in Kok et al. [19,20]. The lower calorific value (LCV) of the oil shale was measured at 6.0 MJ kg^{-1} using a calorimetric bomb.

Around 770 °C, under both air and nitrogen atmosphere, the endothermic peak of decarbonation appears. The measured endothermic reaction heat was – 589 kJ kg^{-1} oil shale.

The experiment performed under N_2 shows that the reaction heat for kerogen devolatilization is too small for a value to be derived.

2.3. Chemical characterization

The oil shale was analyzed by standard elemental analysis (CHONS) using a DIONEX ICS 3000 analyzer. Table 1 shows the compound amounts. It may be noticed that the quantified oxygen amount originates from the organic matter only, because the analyzer does not detect the oxygen contained by mineral matter, which is released as CO_2 during the decarbonation of carbonates.

The standard proximate analysis of oil shale is shown in Table 2. The devolatilization of oil shale yields 2.5% moisture and 26.9% volatile matter, while 6.9% of FC is produced.

It is clear that the results of proximate analysis depend on the conditions used in the procedure. In particular, the heating rate and the conditions of evacuation of volatile matter from the solid particles may affect the results. Since the values obtained from this analysis will be instrumental in establishing a mass balance of the combustion process, detailed proximate analyses were carried out using the horizontal tube furnace, shown in Fig. 5. This reactor consists of a 70 mm i.d. horizontal quartz tube heated electrically and swept by an atmosphere gas that is preheated before reaching the centre of the tube. A 1 mm thick layer of sample was placed in the spoon at the end of a quartz handle and in the cold zone of the reactor out of the hot electrical furnace. The atmosphere was then set to N_2 or to air depending on the test thanks to a continuous

Table 1
CHNSO analysis of oil shale.

	C	H	N	S	O
Oil shale (wt.%)	15.9	1.5	0.24	1.5	10.5
Oil shale residue (wt.%)	1.8	0.1	<0.05	0.68	1.1

Table 2
Standard proximate analysis of oil shale.

Oil shale			
Ash (wt.%)	Volatile (wt.%)	Fixed carbon (wt.%)	Moisture
63.7	26.9	6.9	2.5

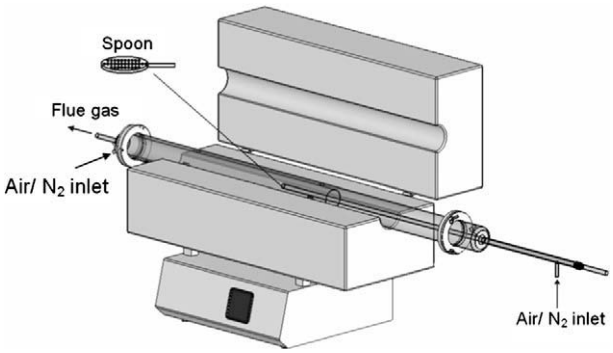

Fig. 5. Horizontal tube furnace.

flowrate of 6 l min^{-1} at STP. The spoon was then pushed to the middle of the furnace, where the temperature was controlled. It was left there for 5 min, and then pulled back to the cold zone and collected after cooling. A thin thermocouple placed besides the sample enabled to evaluate the heating rate undergone by the sample, controlled by inserting the handle more or less rapidly. It was possible to connect the exit of the reactor to a gas bag for *a posteriori* analysis. This apparatus enables the heating rate to be controlled and guarantees an efficient removal of volatile matter from around the particles. When repeating the trials, the repeatability for a mass loss determination was indeed very good: better than 0.4%.

Here, the oil shale is seen as a mix of inert materials, carbonates, organic matter and water, as illustrated in Table 3. From the observation of the thermogravimetric curves, it was decided to operate tests at two temperatures:

(i) at 550 °C, in order to evaluate:

- first, the thermal decomposition (or devolatilization or pyrolysis) of the oil shale, operating under N_2;
- secondly, the oxidation of the FC, shifting the atmosphere to air.

Table 3
Detailed proximate analyses. (–) solids; (....) gas.

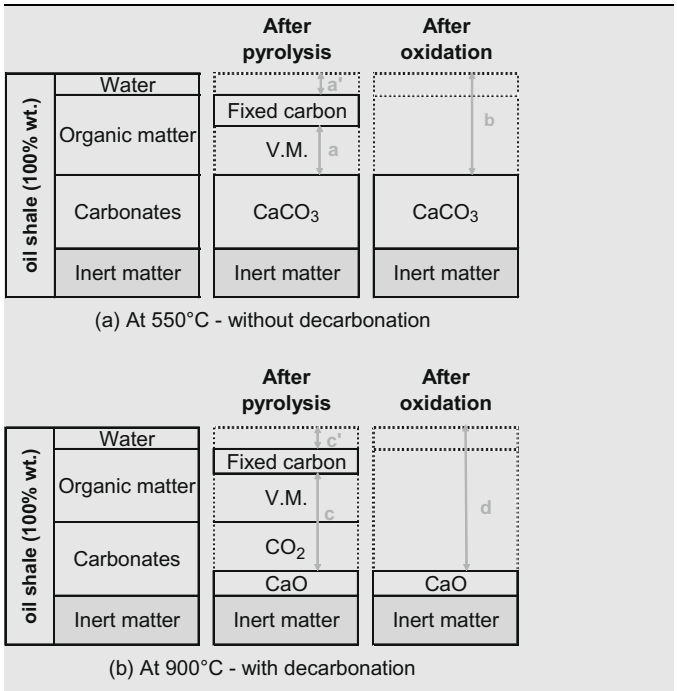

The previous thermogravimetry tests indicated that at this temperature the decarbonation of the carbonates is not achieved within several minutes.

(ii) at 900 °C, in order to obtain the same reactions as in the case of 550 °C testing, but with the occurrence of decarbonation during the thermal decomposition under N_2.

The oil shale decomposition at 550 °C under inert and oxidizing atmospheres makes it possible to determine the amounts of volatile matter and FC, respectively. As illustrated in Table 3a, the amount of volatile matter plus water was $a + a' = 17.2\%$, from which the volatile matter amount is calculated at 14.7% since the amount of water was 2.5%. Shifting the atmosphere from N_2 to air leads to the oxidation of the solid residue of devolatilization, i.e. FC. Therefore, the amount of FC was $b-a-a' = 4.7\%$. This value is very similar to that determined using TGA (4.8%). The value obtained during proximate analysis is higher, at 6.9%. This can be attributed to the fact that during the test, the volatile matter was maintained in contact with the sample inside the test crucible, causing the repolymerization of some volatile matter into solid pyrolytic carbon; this value will not be retained.

At 900 °C, along with the thermal degradation of organic matter, the decarbonation process occurs. The difference $d-c-c'$ gives the amount of FC, determined at 1.2%. It is worth noting that this value is different from that found at 550 °C. This result remains difficult to explain, but confirms the observation made during TG experiments: heating the pyrolyzed oil shale to high temperature (900 °C) under inert atmosphere leads to a progressive decrease in the amount of FC.

Subtracting $d-b$ it is possible to determine the amount of CO_2 produced by decarbonation: about 15.9%. Carbonates can be assumed to be essentially limestone. Considering the decomposition of limestone ($CaCO_3$) into quick-lime (CaO) and carbon dioxide (CO_2) according to the reaction (1), one can determine the amount of $CaCO_3$ as 34.6%.

$$CaCO_{3(s)} \rightarrow 0.56CaO_{(s)} + 0.44CO_{2(g)}$$

This value is similar to the thermogravimetry analysis result, which gave 36.7%.

According to [21], the heating rate has an influence on the product yield in the range 5–40 K min^{-1}. As shown in Martins et al. [15], the oil shale undergoes heating rates in the range 70–90 K min^{-1} along combustion inside the combustion cell. Therefore, using the horizontal tube furnace, the effect of heating rate on the mass loss was investigated. The tests presented above were carried out at a heating rate of 170 K min^{-1}. Two additional tests were carried out at heating rates of 50 and 900 K min^{-1} under N_2. Again, two final temperatures were used: 550 and 900 °C. Table 4 summarizes the results obtained: in the range 50–900 K min^{-1} the heating rate does not affect the mass loss due to pyrolysis (results at 550 °C) and to pyrolysis plus decarbonation (results at 900 °C). Consequently, for particles in the size range 500–1000 μm, the amount of FC was not affected by the heating rate.

Table 5 presents a summary of the results achieved at this stage with some comparison with the literature for Timahdit oil shale.

Table 4
Mass loss of oil shale after heating at 550 °C and 900 °C under N_2, in the horizontal tube furnace following three heating rates.

Heating rate (K min^{-1})			
Furnace temperature (°C)	50	170	900
550	16.5%	17.2%	–
900	36.7%	37.1%	35.9%

Table 5
Summary of composition results of oil shale.

Composition (wt.%)	"Spoon furnace" (170 K min^{-1})	TGA (3 K min^{-1})	Ref. [1]	Ref. [2]
Kerogen	21.9	18.0	24.4	24.3
Carbonates ($CaCO_3$)	34.6	42.3	40.1	35.5
Inert matter	43.5	39.7	35.5	40.5

Table 6
Amounts of pyrolysis gas expressed both as wt.% of the oil shale and in wt.% of organic matter in oil shale.

		Oil shale (wt.%)	Organic matter (wt.%)
Permanent gases	CO	0.20	1.02
	CO_2	0.98	5.05
	SO_2	0.93	4.80
	CH_4	0.37	1.88
	NMHC	1.93	9.93
	H_2	0.01	0.04
	Fixed carbon	4.70	24.23
	Oil = complement	10.28	53
Total		19.4	100.0

The results are similar to those of other authors regarding the composition of the oil shale. The values adopted here were: kerogen 21.9%, $CaCO_3$ 34.6% and Inert matter 43.5%.

2.4. Analysis of the devolatilization gases

In specific experiments using a horizontal tube furnace, the composition of the permanent gases (non-condensable fraction of volatile matter) was established. Since the amount and composition of gases are process dependant, the values obtained here must be taken as estimates. The species CO, CO_2 and H_2 were analyzed using a gas chromatographer. A two-FID detectors analyzer was used to quantify methane and total non-methanic hydrocarbons (NMHC, in equivalent C), while SO_2 was quantified using a NDIR analyzer. The results were expressed first in g/g oil shale, then in g/g of organic matter, as shown in Table 6. Concerning NMHC, a molar mass of 16 g mol^{-1} was assumed for this species (expressed in equivalent mole of carbon). In the table, the mass fractions of FC in oil shale and in the organic matter – as determined previously – were added. A fraction of oil was finally added in the table to recover a total of 100% organic matter; this amount is 53% of the organic matter.

A quarter of organic matter is retrieved as FC; only one quarter of the organic matter is converted into gases, and approximately half of the organic matter is recovered as oil, including some water. NMHC represents approximately 10% of the organic matter initial mass. CO_2 and SO_2 each represent approximately 5%. The species CO represents only 1% of initial organic matter mass, and H_2 is present in negligible quantities. These results will be used further to establish a mass balance of the front propagation process.

3. Products of the combustion

The combustion of oil shale was operated in a specially designed cell described into detail in Martins et al. [15]. Briefly it consists of a stainless steel vertical cylinder of 91 mm i.d. A configuration of 1D co-current downward combustion is retained. At time $t = 0$, the top of the bed (located at $Z = 0$) is ignited thanks to thermal radiation from a cone heater. A grate is placed at the bottom of the reactor ($Z = 300$ mm) to support the fuel. At the bottom of the cell is a flexible tube connected to reservoirs to condense and collect liquid oil. The air entry is designed to supply uninterrupted controlled airflow in a symmetrical way. Gas analyzers can be momentarily connected at the exit of the condensers to quantify produced gas. In order to avoid the deterioration of the reactor wall due to excessive temperature, a mixture of oil shale and sand 75/25 wt. was used in the experiments. The sand particle size range was also 500–1000 μm; it was checked that the mass loss of the sand heated at 1000 °C under air was negligible: 0.26%. The apparent density of the packed bed mixture OS/sand was 1168 kg m^{-3}. The porosity of the bed was consequently 47.2% (the real density of the sand was 2447 kg m^{-3}).

A mass of 2127 g of mix 75/25 wt. oil shale/sand was introduced in the cell. The experiments were run with co-current air supply in downdraft batch experiments. An air flow rate of 9.5 l min^{-1} at STP was used; this corresponds to a flow rate of 1460 l min^{-1} at STP for 1 m^2 of section, and to a Darcy velocity of 0.024 m s^{-1} at 20 °C, or 0.108 m s^{-1} at 1000 °C. The solid residue was recovered, and the flue gases were analyzed. Details for these experiments can be found in Martins et al. [15].

3.1. Observation and analysis of the solid residue

The solid residue (of oil shale + sand) after combustion homogeneously occupied all the volume of the cell; its apparent density was 956.9 kg m^{-3}. No liquid oil deposited at the surface of the grains or impregnating the grains was observed. The particles were not sticky and were odorless, while the flue gases had a very strong smell.

Detailed analysis of the solid residue mix was carried out.

- The mass loss under air at 550 °C was found at 0.622%, corresponding to the residual FC amount.
- At 1000 °C the mass loss - including residual FC oxidation and decarbonation of the residual carbonates – was 3.5%. The mass loss of CO_2 was then 2.88%, which is equivalent to a residual amount of $CaCO_3$ of 6.543%.

A synthesis of these results is presented in Fig. 6. On the left-hand side, the composition of raw oil shale is re-stated. The two vertical bars at the centre establish a link between the masses of components in 100 g of oil shale/sand mix before combustion, which lead to 74.5 g of solid residue after combustion. On the right-hand side, the composition of oil shale residue is given, excluding sand. It can be calculated that the front, at its passage:

– dries the oil shale, which was expected;
– devolatilizes the organic fraction;
– oxidizes 88.2% of the FC that is formed (4.7% of the initial oil shale);
– decarbonates 83.2% of the initially present carbonates (34.66% of oil shale).

The final mass loss of the oil shale was 33.0%. The oil shale residue after combustion contained 0.84% of FC, 8.82% of CaCO3, 24.4% of CaO and 65.82% of inert.

Ultimate analyses were then performed on the solid residue. The amount of C was 1.8%, which is compatible (taking measurement errors into account) with the value of 0.84% determined previously. H was found at 0.1% and O at 1.1%, confirming that devolatilization was completed. Less than 0.05% N and 0.68% S were found. The O content is 1.1%. Again the O contained by the residual $CaCO_3$ is not taken into account by the measurement.

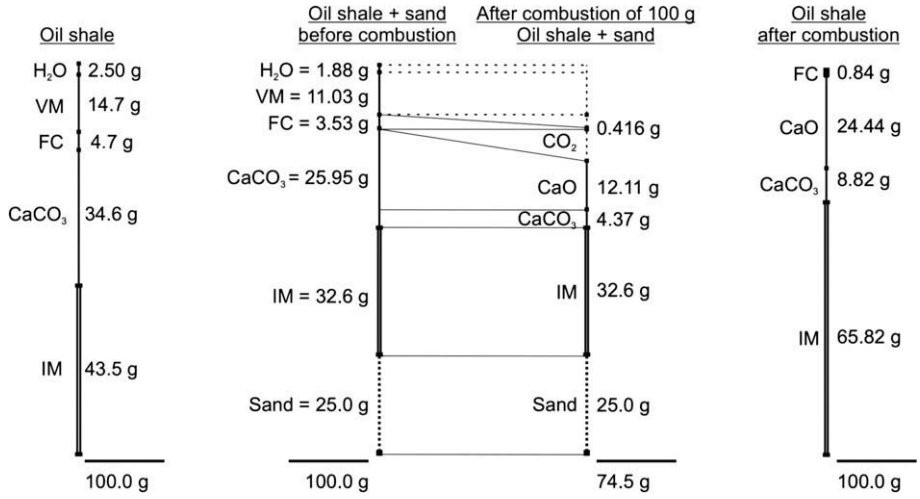

Fig. 6. Synthesis of the characterization of oil shale and oil shale after combustion. Where: volatile matter (VM), fixed carbon (FC) and inert matter (IM).

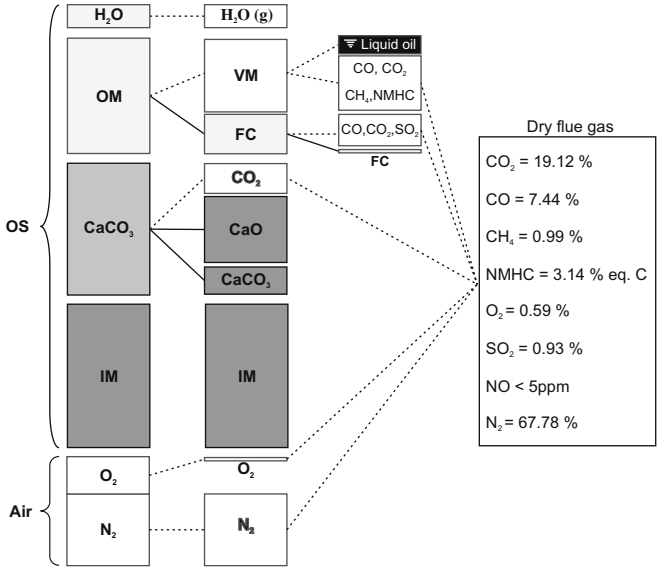

Fig. 7. Description of the conversion of oil shale and air to produce the flue gas. On a dark color the components of OS solid residue.

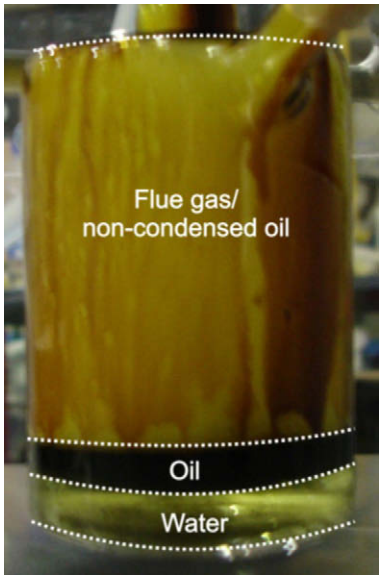

Fig. 8. Shale oil recovery during experiments.

3.2. Observation and analysis of the flue gas

The smoke was transparent until the front reached $Z = 180$ mm; it then started to change color to a dense white, and condensation of water appeared inside the tubes. A few minutes after that, the smoke became yellow and at the same time, the first oil drops fell down inside the container.

Fig. 7 illustrates the transformations of oil shale and the reaction with air to form the flue gas, indicating the origin of each species. It also reports the results from analysis of the dry flue gas. It is reminded here that the products of combustion are strongly process dependant; they can be affected by the propagation mode, sample size, heating rate, temperature level and incoming flow composition and velocity.

The amount of oxygen is small: 0.59% when air (20.86% O_2) was supplied. This indicates that the front consumes almost all of the oxygen, and is therefore limited in velocity by oxygen supply. This is the expected situation for smoldering.

The amount of methane is 0.99%, that of NMHC of 3.14% (equivalent C) and that of CO 7.44%. From this, and assuming that the NMHC has the same LCV as methane, the LCV of the flue gas can be calculated at 54 kJ mol^{-1} from the molar fractions of fuel gases in the flue gas and from their LCV.

3.3. Liquid oil produced

At the end of the experiment, liquid oil was recovered in the reservoir; see Fig. 8. The oil tended to be separated into different phases. Clear water was observed at the bottom, while a second black phase was floating; a third very viscous phase lay at the bottom. The analysis of oil is complex: hundreds of components are typically present. It was not undertaken in this work.

After separation from clear water, the mass of oil was 160 g. In other words 52% of the mass of organic matter initially present in oil shale is recovered as oil. It is interesting to note that this value is in agreement with the amount of formed oil deduced from characterization of devolatilization gases, 53%. Nevertheless, this correspondence should not be considered as trivial, since the oil formed in the combustion cell at pyrolysis may be cracked downstream into permanent gas or oxidized.

3.4. Instantaneous mass balance of the process

The mass balance established here consists in calculating the composition of the flue gas coming out of the cell. The calculated values will be compared with the values measured experimentally. One can expect two types of results from an instantaneous mass balance:

(i) Several clues can be found in the investigation of what is actually oxidized – part of the FC and potentially part of volatile matter – during the front propagation.
(ii) It should be possible to determine the respective proportions of CO and of CO_2 resulting from FC oxidation.

As illustrated in Fig. 7, the flue gas contains:

- the N_2 flow of the inlet air flow;
- the O_2 flow of the inlet airflow that was not oxidized;
- H_2O resulting from the drying of oil shale;
- CO_2 and CO resulting from:
  - direct production of the devolatilization;
  - the oxidation of part of the FC, following the reaction: $C + [\frac{fr}{2} + (1-fr)]O_2 \rightarrow fr\,CO + (1-fr)CO_2$ where fr is an adjustable parameter to balance the ratio of the products of combustion CO and CO_2.
- CO_2 resulting from the decarbonation of carbonates;
- Volatile matter: liquid oil and devolatilization gases (CO, CO_2, CH_4, NMHC).

During the experiment, and at time t = 2079 s, the front was located at Z = 90 mm (thermocouple 3), and gases were sampled and analyzed. The front velocity was 3.68 mm min^{-1}. From this, the mass balance was established as follows:

- we consider here that there is no oxidation of volatile matter and of oil, as indicated in the literature for co-current smoldering;
- the flow rates of devolatilization gases, of oil, and of formed FC were calculated using the partitioning established in the analysis of the devolatilization gases;
- a fraction of 88.2% of the FC – as determined previously - was allowed to react with oxygen from the air supply;
- 83% of the carbonates were decarbonated as determined previously in this work.
- the molar composition of the flue gas was calculated, and is reported in Table 7.

3.4.1. Results

Fixing the f_r coefficient at 0.565, the fractions of CO and CO_2 calculated from the mass balance are in very good agreement with the experimentally measured fractions. This indicates that 56.5% of this carbon is finally retrieved as CO, while the rest is converted to CO_2. The assumption that there is no oxidation of volatile matter is verified *a posteriori* since the calculated amounts of CH_4 and NMHC correspond with experimental measurements. This indicates that these species, once formed during the devolatilization, are driven out of the cell without significant transformation. Finally, it can be concluded that the front propagation is sustained by the oxidation of part of the FC only. This situation has been observed by previous authors and is characteristic of smoldering [4,22].

Considering the amounts of CO_2 that are formed, it can be established from this mass balance that CO_2 from decarbonation of carbonates represents 69% of the total CO_2 emissions, i.e. including CO_2 from FC oxidation. Consequently, the decarbonation has a strong environmental impact in terms of CO_2 emissions.

If one considers the mass balance of oxygen species, the calculation predicts 6.66% residual O_2 in the flue gas, while 0.59% is found experimentally. This would suggest that some O_2 has been consumed by another reaction not considered here. This reaction might be the LTO identified during DSC experiments, where a first exothermic peak was observed before the char oxidation peak. Ohlemiller [4] pointed out that this reaction - also called oxidative pyrolysis - is an exothermic adsorption of O_2 by the sample, and is an appreciable heat source in many smoldering processes. Additional tests were performed and support this explanation. Some oil shale was previously devolatilized, to produce a semicoke that contained less than 1% VM, instead of 14.7% for oil shale. The smoldering of semicoke was performed in the cell and in the same conditions as for the oil shale. In this case, the oxygen balance was closed with less than 1% O_2 in the flue gas deviation. In the case of semicoke smoldering, the LTO reaction could not occur, enabling to close the oxygen balance. The improvement of the mass balance of oxygen species will be subject to future study in the context of this project.

An energy balance can be established, based on:

- the LCV of the oil shale – measured at 6.0 MJ kg^{-1} using a calorimetric bomb;
- the energy contained in the flue gas;
- the energy consumed by FC oxidation.

The oxidation of FC into CO and CO_2 consumes 10% of the energy contained by the oil shale, while the FC left in the oil shale residue represents only 2.3%. The flue gas calorific value energy represents 17% of the oil shale energy.

Table 7
Composition of the flue gas (vol.%) as determined from analysis and as calculated from the mass balance.

	From experiments	From mass balance
O_2	0.59	6.66
CO	7.44	7.44
CO_2	19.12	19.18
CH_4	0.99	0.88
NMHC	3.14	3.70
N_2	–	60.72

4. Conclusion

Timahdit oil shale contains 2.5% moisture and produced 14.7% VM when heated at 550 °C. The oil shale also contains 34.6% carbonates and 43.5% of inert materials.

The amount of FC – that supports the front propagation – was around 4.7% of the initial mass of OS according to repeated tests in the Horizontal Tube Furnace at 550 °C. For particles in the size range 500–1000 μm, it is shown to remain constant when the heating rate is varied between 50 and 900 K min^{-1}.

The passage of the combustion front in the mix 75/25 wt. of OS/sand with an air supply of 1460 l min^{-1} m^{-2} STP was characterized. The front induces full devolatilization of organic matter into FC and VM. Globally, part of the VM is condensed: approximately 52% of the organic matter of the OS is recovered as liquid oil.

The solid residue after combustion is not totally free of organic matter since not all the FC is oxidized: the OS residue contains 0.84% of C. The flue gas is a calorific gas: its LCV is 54 kJ mol^{-1}. It contains 17% of the energy initially present in OS. Its composition was established at 7.44% CO, 3.14% non-methanic hydrocarbons and 0.99% CH_4.

A fraction of 56.5% of the fixed carbon oxidizes to CO and the rest to CO_2.

Finally, the front induces the decarbonation of 83% of the initially present carbonates. The CO_2 so formed represents 69% of the total emitted CO_2. If OS had not been diluted with sand, the combustion temperature would have been higher, as would the decarbonation rate. It may be possible to avoid this CO_2 release by maintaining low temperature conditions, where decarbonation is not promoted; whether a combustion front can be propagated in such conditions is a question open to further research work.

Another perspective remains open to research if the aim is to increase the efficiency of an oil/gas recovery process: decreasing the fraction of FC that is oxidized to CO_2 – in order to increase the CO production.

Acknowledgements

We thank Mr. Chrifa of ONIM Morocco for supplying the oil shale samples used in this work.

References

[1] Saoiabi A, Doukkali A, Hamad M, Zrineh A, Ferhat M, Debyser Y. Schistes bitumineux de Timahdit (Maroc): composition et propriétés physicochimiques Timahdit (Morocco) oil shales: composition and physicochemical properties. Comptes Rendus de l'Académie des Sciences - Series IIC – Chemistry 2001;4(5):351–60.
[2] Sadiki A, Kaminsky W, Halim H, Bekri O. Fluidized bed pyrolysis of Moroccan oil shales using the hamburg pyrolysis process. J Anal Appl Pyrolysis 2003;70(2):427–35.
[3] Palmer KN. Smoldering combustion in dusts and fibrous materials. Combust Flame 1956;1:129–54.
[4] Ohlemiller TJ. Modelling of smoldering combustion propagation. Prog Energy Combust Sci 1985;11:277–310.
[5] Rein G. Smouldering combustion phenomena in science and technology. Int Rev Chem Eng 2009;1(1):3–18.
[6] Ziyad M, Garnier J-PP, Halim M. Nonisothermal kinetics of H_2S and H_2 generation from Timahdit oil shale. Fuel 1986;65(5):715–20.
[7] Chanaa MB, Lallemant M, Mokhlisse A. Pyrolysis of Timahdit, Morocco, oil shales under microwave field. Fuel 1994;73(10):1643–9.
[8] Ichcho S, Khouya E, Fakhi S, Ezzine M, Hannache H, Pallier R, Naslain R. Influence of the experimental conditions on porosity and structure of adsorbents elaborated from Moroccan oil shale of Timahdit by chemical activation. J Hazard Mater 2005;118(1–3):45–51.
[9] Akash BA, Jaber JO. Characterization of shale oil as compared to crude oil and some refined petroleum products. Energy Sources 2003;25(12):1171–82.
[10] Tiikma L, Tamvelius H, Luik L. Coprocessing of heavy shale oil with polyethylene waste. J Anal Appl Pyrolysis 2007;79:191–5.
[11] Luik H, Luik L, Tiikma L, Vink N. Parallels between slow pyrolysis of Estonian oil shale and forest biomass residues. J Anal Appl Pyrolysis 2007;79:205–9.
[12] Ots A, Arro H, Pihu T, Prikk A. Behavior of carbonate-rich fuels in ACFBC and PFBC conditions. In: Proceedings of the 15th international conference on fluidized bed combustion. 1999.
[13] Ots A, Pihu T, Hlebnikov A. The influence of pressure on the behavior of fuel carbonates. US: Springer; 2002, p. 685–95.
[14] EASAC. A study on the EU oil shale industry – viewed in the light of the Estonian experience. A report by EASAC to the committee on industry, research and energy of the European Parliament, 2007.
[15] Martins MF, Salvador S, Thovert J-F, Debenest G. "Co-current combustion of oil shale – Part 2: Structure of the combustion front". Fuel 2009;89(1):133–43.
[16] Rajeshwar K, Nottenburg R, Dubow J. Thermophysical properties of oil shales. J Mater Sci 1979;14(9):2025–52.
[17] Kok MV. Heating rate effect on the DSC kinetics of oil shales. J Therm Anal Calorim 2007;90(3):817–21.
[18] Rein G, Bar-Ilan A, Fernandez-Pello AC, Ellzey JL, Torero JL, Urban DL. Modeling of one-dimensional smoldering of polyurethane in microgravity conditions. Proc Combust Inst 2005;30(2):2327–34.
[19] Kok MV, Sztatisz J, Pokol G. Characterization of oil shales by high pressure DSC. J Therm Anal Calorim 1999;56:939–46.
[20] Kok MV, Pamir R. Non-isothermal pyrolysis and kinetics of oil shales. J Therm Anal Calorim 1999:953–8.
[21] Williams PT, Ahmad N. Influence of process conditions on the pyrolysis of Pakistani oil shales. Fuel 1999;78(6):653–62.
[22] Torero JL, Fernandez-Pello AC. Forward smolder of polyurethane foam in a forced air flow. Combust Flame 1996;106(1–2):89–109.